Highly Efficient Integrated Generator of Tripartite Entanglement from $\chi^{(2)}$ Whispering Gallery Microresonator

Guangqiang He, Linxi Hu & Rongyu Li

International Journal of Theoretical Physics

ISSN 0020-7748
Volume 56
Number 8

Int J Theor Phys (2017) 56:2458-2466
DOI 10.1007/s10773-017-3397-4

Springer

Int J Theor Phys (2017) 56:2458–2466
DOI 10.1007/s10773-017-3397-4

Highly Efficient Integrated Generator of Tripartite Entanglement from $\chi^{(2)}$ Whispering Gallery Microresonator

Guangqiang He[1,2,3] · Linxi Hu[1] · Rongyu Li[1]

Received: 9 January 2017 / Accepted: 18 April 2017 / Published online: 28 April 2017

Abstract Whispering gallery microresonator (WGM) filled with nonlinear material has proven to be valuable for enhancing nonlinear optical effects. Here we explore the production of the pump-signal-idler tripartite entanglement based on the integrated high-Q whispering gallery mode cavities filled with lithium niobate. Our theoretical analysis about the entanglement condition when the van Loock and Furusawa criteria are violated paves the way for future investigation of integrated entanglement based on nonlinear high-Q microresonator. In addition, we present parameters used in our designed generator and our theoretical model is highly expansible to further exploration of entanglement over general $\chi^{(2)}$ whispering gallery microresonator.

Keywords High-Q $\chi^{(2)}$ whispering gallery microresonator · Tripartite entanglement

1 Introduction

Quantum computation is expected to provide exponential speedup for particular mathematical problems such as integer factoring, quantum system simulation and quan-

✉ Guangqiang He
gqhe@sjtu.edu.cn

1 State Key Laboratory of Advanced Optical Communication Systems and Networks, Department of Electronic Engineering, Shanghai Jiao Tong University, Shanghai 200240, China

2 State Key Laboratory of Precision Spectroscopy, East China Normal University, Shanghai 200062, China

3 State Key Laboratory of Information Security, Institute of Information Engineering, Chinese Academy of Sciences, Beijing 100093, China

tum information processing [1]. Quantum cryptographic communication, on the other hand, provides an absolutely safe way to pass information without the risk of eavesdropping [2].

In the center of both quantum computation and quantum communication lies the concept of quantum entanglement, therefore the generation of multipartite entanglement always draws wide attention. Many works are related to this field [3–8]. Conventionally, entangled photon pairs are generated in $\chi^{(2)}$ bulky crystals that are usually difficult to operate and susceptible to environmental perturbations. It is recently proposed that entangled photon pairs can also be generated from monolithic microresonators of whispering-gallery type [6] via four-wave mixing (FWM) processes in $\chi^{(3)}$ materials [7] and all optical squeezing in an on-chip monolithically integrated complementary metal oxide semiconductor (CMOS) compatible platform is observed [8].

In a whispering-gallery resonator, whispering-gallery modes of discrete propagation constant are guided by continuous total internal reflection along a curved surface. WGM resonators have the strengths of high confinement to the optical field, exceptionally high quality factor, and compatibility to compact, chip-scale integration, so they have been replacing $\chi^{(2)}$ bulky crystals in many other applications of laser optics recently [9–12].

The $\chi^{(2)}$ parameter is usually about two orders higher than $\chi^{(3)}$, so the former paradigm enjoys a much more significant nonlinear effect, and therefore, achieves entanglement more easily. In this paper, we propose a theoretical model for generation of a tripartite quantum entanglement from a whispering gallery mode, and exhibit the design parameters over $\chi^{(2)}$ medium, paving the way for future optical quantum computation on chips.

2 System Model

Our generator scheme is shown in Fig. 1. A narrow linewidth tunable CW laser followed by EDFA and BPF is continuously pumped into the microresonator to intrigue nonlinear effect in the whispering gallery mode cavity filled with lithium niobate (LN). PC is used to control the polarization of input pump laser. Once the nonlinear effect produces different frequencies photons compared with pump wave, we could utilize AWG to separate these beams to analyse their characteristics. The ring cavity is used for our entanglement detection [13].

The resonator we used is a integrated cavity filled with LN medium and the original photons annihilation and new photons occurrence originate from spontaneous parametric down conversion (SPDC) effect. The coupling coefficient g of our system is

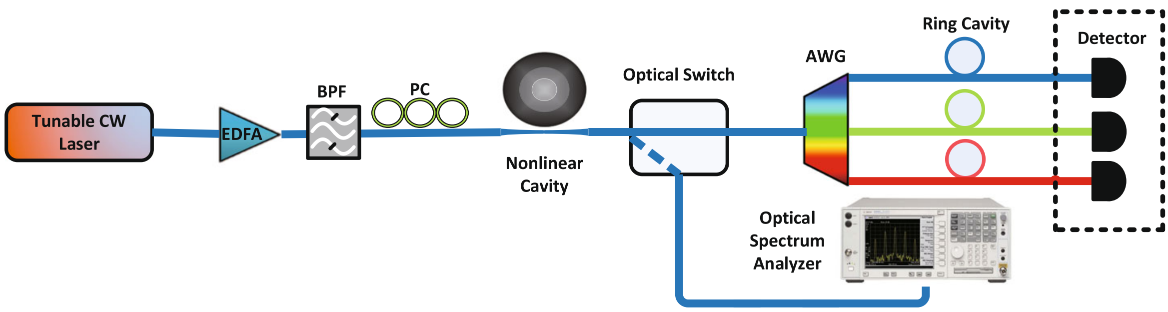

Fig. 1 Tripartite entanglement generator with LN WGM and angle-polished fiber coupling. Tunable CW Laser, Tunable continuous-wave laser; EDFA, Erbium-doped fiber amplifier; BPF, bandpass filter; PC, polarization controller; AWG, arrayed waveguide grating

$g = 2\pi\omega_s \frac{\chi^{(2)}}{\varepsilon_s}\frac{V_{sip}}{V_s}\sqrt{\frac{2\pi\hbar\omega_p}{\varepsilon_p V_p}}$ [14]. Once we determine the coupling coefficient, the Hamiltonian for our system is found to be

$$H = H_{pump} + H_{int} + H_{free}, \tag{1}$$

$$H_{pump} = i\hbar a_p^\dagger \varepsilon_p + H.c., \tag{2}$$

$$H_{int} = i\hbar\left(g a_p a_s^\dagger a_i^\dagger\right) + H.c., \tag{3}$$

$$H_{free} = \hbar\sum_k \omega_k a_k^\dagger a_k. \tag{4}$$

Due to the momentum conservation among the interacting photons, microresonator converts the pump wave into two different frequency waves $\omega_p \rightarrow \omega_s + \omega_i$. Besides, in the microresonator, there might be other sorts of nonlinear effect happens. However, owing to the smaller intensities and larger phase mismatch, we thus neglect those processes in our analysis.

A microresonator is an open system since it not only exhibits intrinsic scattering loss with a photon decay rate of γ_{k0} (for mode k), but also couples waves to the coupling waveguide with an external coupling rate of γ_{kc}. In order to describe such an open system, we present the loss and out-coupling terms as

$$L_k\rho = \gamma_k\left(2a_k\rho a_k^\dagger - a_k^\dagger a_k\rho - \rho a_k^\dagger a_k\right), \tag{5}$$

where ρ stands for the density matrix of system and $\gamma_k = \gamma_{kc} + \gamma_{k0}$ represents the damping rate of the loaded cavity. Then the output field is determined by the well-known input-output relation given as [15]

$$b_{out} - b_{in} = \sqrt{\gamma}a \tag{6}$$

in which b is the boson annihilation operator for the bath field outside the cavity.

3 Equations Of Motion For The Full Hamiltonian

As for the system model presented previously, whole procedure could be governed by the following master equation

$$\frac{\partial\rho}{\partial t} = -\frac{i}{\hbar}[H_{pump} + H_{int}, \rho] + \sum_{k=1}^{3} L_k\rho. \tag{7}$$

The free Hamiltonian has been omitted here in (7) because of adding an rotating-wave approximation$e^{-\omega_k t}$ in it [15].

To solve the master equation, we consort the Fockker-Planck equation in P representation which could be shown as a stochastic differential equation [16]

$$\frac{\partial\alpha}{\partial t} = F + B\eta, \tag{8}$$

where $\alpha = [\alpha_p, \alpha_s, \alpha_i, \alpha_p^*, \alpha_s^*, \alpha_i^*]^T$ and $F = [f, f^*]^T$ stands for the main part of the system evolution. f is given as

$$f = \begin{pmatrix} g\alpha_s\alpha_i - \varepsilon_p + \gamma_p\alpha_p \\ -g\alpha_p\alpha_i^* + \gamma_s\alpha_s \\ -g\alpha_p\alpha_s^* + \gamma_i\alpha_i \end{pmatrix}.$$

Matrix B is the noise terms which could be obtained by the relationship $BB^T = D$. D matrix we introduced here stands for the diffusion matrix, which is given by

$$D = \begin{pmatrix} d & 0 \\ 0 & d^* \end{pmatrix},$$

where d is given by

$$d = \begin{pmatrix} 0 & 0 & 0 \\ 0 & 0 & g\alpha_p \\ 0 & g\alpha_p & 0 \end{pmatrix}.$$

In (8), $\boldsymbol{\eta} = [\eta_1(t), \eta_2(t), \eta_3(t), c.c]^T$, where η_i are real noise terms which is determined by $\langle \eta_i(t) \rangle = 0$ and $\left\langle \eta_i(t)\eta_j(t) \right\rangle = \delta_{ij}\delta(t-t')$.

4 Linearized Quantum-Fluctuation Analysis

In order to solve (8), we convert the system variables into their steady-state(classical) values and quantum fluctuations as $\alpha_k = A_k + \delta\alpha_k$. Due to the facts that quantum fluctuations are enough small compared with steady-state, thus it's reasonable for us to utilize the linearisation analysis to find the spectra for the cavity outputs. To simplify the calculation, we assume the s and i photons share the same photon decay rate and identical coupling coefficient ($\gamma_s = \gamma_i, \gamma_{sc} = \gamma_{ic}, \gamma_{s0} = \gamma_{i0}$). And A_s indicates the steady state for signal wave and A_i is on behalf of idler wave steady state. As a result, (8) could be rewritten as owing to assumption that $\frac{\partial A}{\partial t} = 0$,

$$\frac{\partial A + \delta\alpha}{\partial t} = \frac{\partial \delta\alpha}{\partial t}, \tag{9}$$

$$\frac{\partial \delta\alpha}{\partial t} = F + B\eta = f(A) + f(A, \delta) + B\eta. \tag{10}$$

Firstly we complete the steady-state solution by setting the $f(A) = 0$. $f(A)$ is given below,

$$f(A) = \begin{pmatrix} gA_sA_i - \varepsilon_p + \gamma_p A_p \\ -gA_pA_i^* + \gamma_s A_s \\ -gA_pA_s^* + \gamma_i A_i \\ gA_s^*A_i^* - \varepsilon_p + \gamma_p A_p^* \\ -gA_p^*A_i + \gamma_s A_s^* \\ -gA_p^*A_s + \gamma_i A_i^* \end{pmatrix}.$$

The pump threshold is given by $\varepsilon_{th} = \gamma_p \frac{\sqrt{r_s r_i}}{g}$. When $\varepsilon < \varepsilon_{th}$, the steady states are given as

$$A_p = \varepsilon/\gamma_p, \tag{11}$$

$$A_s = 0, \tag{12}$$

$$A_i = 0. \tag{13}$$

When $\varepsilon > \varepsilon_{th}$, the steady states are given as

$$A_p = \frac{\sqrt{r_s r_i}}{g}, \tag{14}$$

$$A_s = \sqrt{\frac{(\varepsilon - r_p A_p) r_i}{g^2 A_p}}, \tag{15}$$

$$A_i = \frac{g A_p A_s}{r_i}. \tag{16}$$

Notice that, there is a threshold for pump wave and if the pump wave power is below the threshold, there would be no steady solution for signal wave and idler wave. Thus here we only consider the situation that the field modes oscillate above the threshold.

Once we get the steady states outcomes for each photon mode, we put them back into the (8) and get the new simplified equation

$$\frac{\partial \delta\alpha}{\partial t} = f(A, \delta) + B\eta = M\delta\alpha + B\eta \tag{17}$$

in which $\delta\alpha = [\delta\alpha_p, \delta\alpha_s, \delta\alpha_i, \delta\alpha_p^*, \delta\alpha_s^*, \delta\alpha_i^*]^T$. M is the drift matrix given by

$$M = \begin{pmatrix} m_1 & m_2 \\ m_2^* & m_1^* \end{pmatrix},$$

where m_1 and m_2 is

$$m_1 = \begin{pmatrix} \gamma_p & gA_i & gA_s \\ -gA_i & \gamma_s & 0 \\ -gA_s & 0 & \gamma_i \end{pmatrix},$$

$$m_2 = \begin{pmatrix} 0 & 0 & 0 \\ 0 & 0 & -gA_p \\ 0 & -gA_p & 0 \end{pmatrix}.$$

For the validity of linearised quantum-fluctuation analysis, the quantum-fluctuation must be small enough compared with mean values. If the requirement that the real part of the eigenvalues of $-M$ stay non-negative is satisfied, the fluctuation equations will describe an Ornstein-Uhlenbeck process [17], for which the intracavity spectral correlation matrix is given by

$$S(\omega) = (-M + i\omega I)^{-1} D(-M^T - i\omega I)^{-1}. \tag{18}$$

This matrix involves all the correlations required to study the measurable extracavity spectra and we have checked the stability numerically in the rest of discussion.

We introduce the quadrature operators for each mode in order to discuss the tripartite entanglement

$$X_k = a_k + a_k^\dagger, \tag{19}$$

$$Y_k = -i\left(a_k - a_k^\dagger\right), \tag{20}$$

with a commutation relationship of $[X_k, Y_k] = 2i$. Thus we know that $V(X_k) \leq 1$ could stand for the squeezed state based on our operator definition. $V(A) = \langle A^2 \rangle - \langle A \rangle^2$ indicates the variance of operator A.

The output fields are determined by the well-known input-output relations (6). In particular, the spectral variances and covariances have the general form

$$S^{out}_{X_i}(\omega) = 1 + 2\gamma_c S_{X_i}(\omega), \tag{21}$$
$$S^{out}_{X_i,X_j}(\omega) = 2\gamma_c S_{X_i,X_j}(\omega), \tag{22}$$

Y quadratures have the similar expressions.

Multipartite entanglement criteria is given by the van Loock and Furusawa(VLF) [18]. In our discussion, we consider Fokker-Planck equation in P representation and then analyse the entanglement condition that van Loock and Furusawa criteria are violated simultaneously. By using the above quadrature definitions, the tripartite criteria is given by

$$S_{(1)} = V(X_s - X_i) + V(Y_s + Y_i - g_p Y_p) \geq 4 \tag{23}$$
$$S_{(2)} = V(X_p + X_s) + V(Y_p - Y_s - g_i Y_i) \geq 4 \tag{24}$$
$$S_{(3)} = V(X_p + X_i) + V(Y_p - Y_i - g_s Y_s) \geq 4 \tag{25}$$

in which g_k are arbitrary real parameters that are used to optimize the violation of these inequalities. Notice that, the frequencies of signal wave and idler wave are almost same compared with the pump wave, thus we choose to investigate S_1 and S_2 in our rest analysis.

Our microresonator is a spherical cavity of radius $R = 1.5$ mm, thickness $d = 0.5$ mm, filled with lithium niobate medium. The coupling coefficient of our system is $g = 2\pi\omega_s \frac{\chi^{(2)}}{\varepsilon_s} \frac{V_{sip}}{V_s} \sqrt{\frac{2\pi\hbar\omega_p}{\varepsilon_p V_p}}$ [14], in which $\omega_s = 1.94 \times 10^{14}\ s^{-1}$, $\omega_p = 3.87 \times 10^{14}\ s^{-1}$, $V_p \approx 2\pi R \times 2R\sqrt{\left(\frac{2\pi}{\upsilon_p}\right)} \times \frac{R}{\upsilon_p^{2/3}} = 10^{-6}\ cm^3$, and $\chi^{(2)} = 7 \times 10^{-10}$cgs, $V_{sip}/V_s = 0.3$. Besides that, loaded Q factors are $Q_p \simeq 8 \times 10^6$, $Q_s \simeq 1.2 \times 10^7$. The wavelength of the pump beam is $\lambda_p = 775$ nm in the vacuum and wavelength of signal beam is $\lambda_s = 1548$ nm, idler beam is $\lambda_i = 1552$ nm.

Our coupling coefficient for $\chi^{(2)}$ is 0.0136 around, larger about two orders than $\chi^{(3)}$ coupling coefficient [7], which is about 1.09×10^{-4}, proving its highly efficiency.

5 Output Fluctuation Spectra

From our above discussion in Eq. [8–16], the stable solution is completely governed by three parameters: total damping rate γ, coupling coefficient g, and pump wave power ε, which in turn determine the drift matrix M, the diffusion matrix D, and the intracavity spectral correlation matrix S.

To begin with, we fixed the pumping power ε, but it's always the variables outside the cavity that we observe. Thus the transfer also plays a role in the observation, which is determined by a ratio γ_c/γ. We vary the ratio based on the fixed other components to investigate its influence over tripartite entanglement. In Fig. 2, we plot the minimum of the variances versus the analysis frequency normalized to γ when γ_c sets to the portion of 0.09, 0.34, 0.8 and 1 of the total damping rate. Due to fact that signal photon has the similar characteristic with idler photon, we choose to focus on the $S_{(1)}$ and the $S_{(2)}$. The red dashed one relate with $S_{(1)}$ while blue solid one stands for $S_{(2)}$.

It's important to notice from figure that when $\gamma_c/\gamma = 0.09$, there is no entanglement between pump photon and signal photon. As we increase the out-coupling coefficients, the s starts to entangle with p around the center frequency until $\gamma_c/\gamma = 0.34$. And eventually

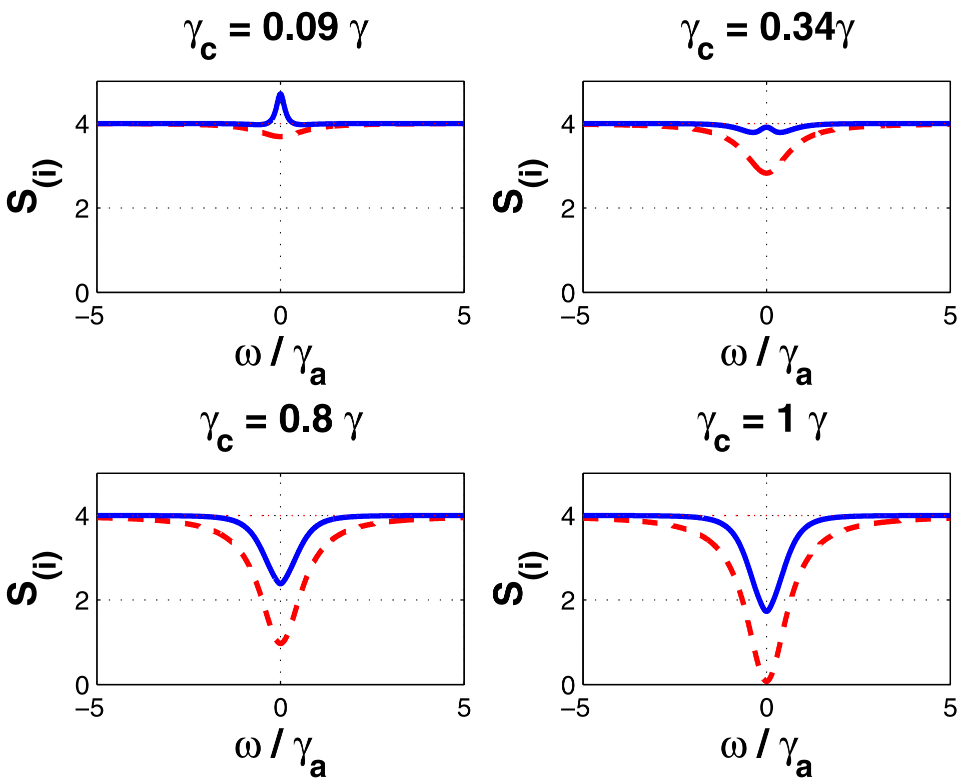

Fig. 2 Four variances versus frequency of pump plots when γ_c/γ is 0.09, 0.34, 0.8, 1. The pump power is fixed at $1.2\varepsilon_{th}$

when we set the portion to the $\gamma_c/\gamma = 1$, the degree of entanglement is the largest compared with other case. As a result, we conclude that the entanglement among output modes increased as the term γ_c/γ. And the higher portion the coupling coefficient is, the less consumed entangled pairs are wasted in the internal loss. Therefore, the entanglement would be better when the cavity has lower intracavity loss and higher extracavity coupling coefficient.

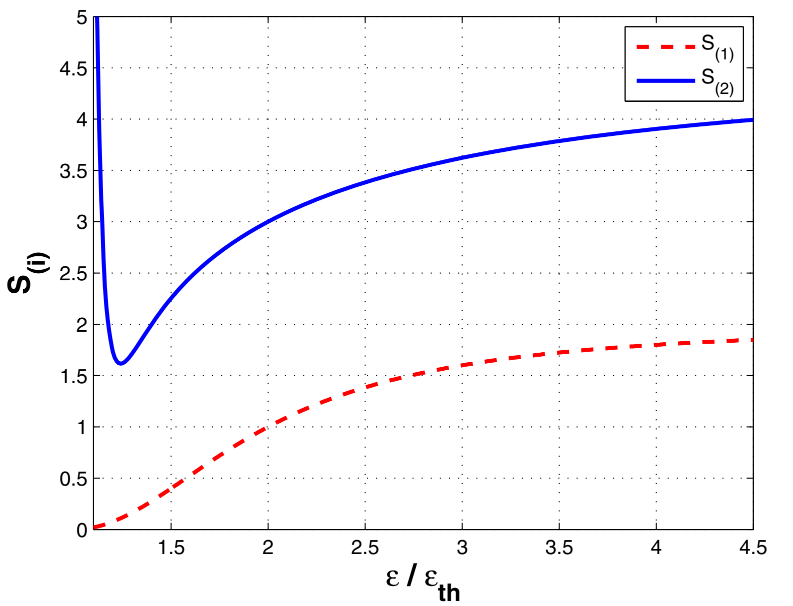

Fig. 3 The minimum variance as a function of pump power. The external coupling coefficient is fixed at $\gamma_c = \gamma$

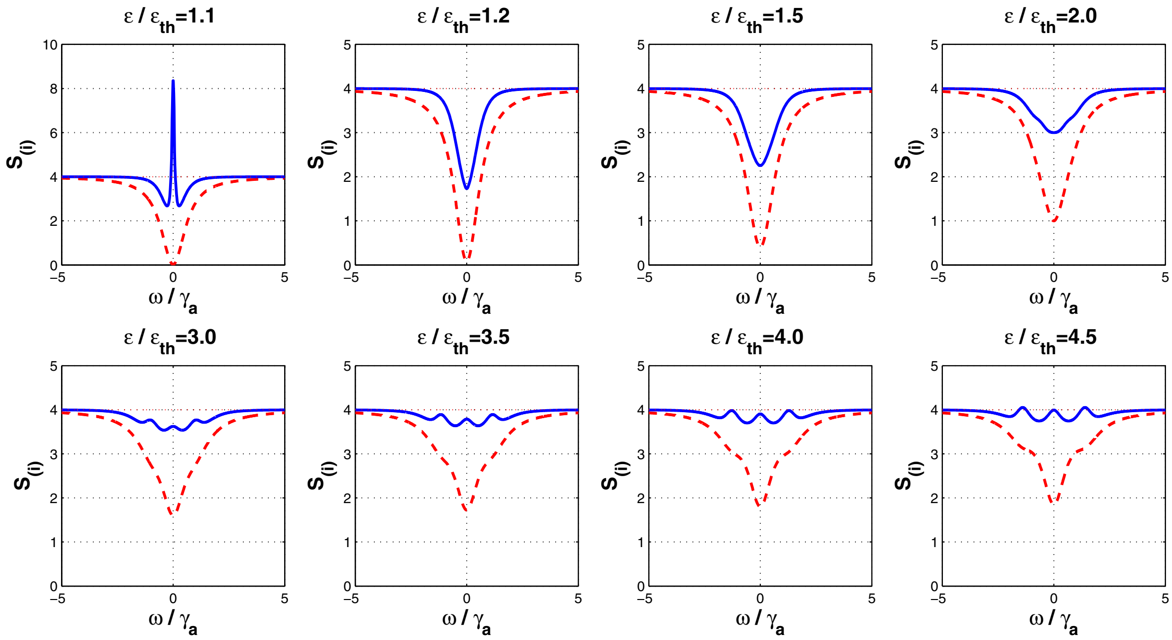

Fig. 4 Extracavity variance versus frequency of pump power. The external coupling coefficient is fixed at: $\gamma_c = \gamma$

In order to investigate the effect the pump power bringing to the degree of entanglement, we firstly set the $\gamma_0 = 0$ which means no intracavity loss in this part of discussion. With our previous discussion, the variance $S_{(i)}$ as a function of ω/γ is merely determined by the parameter $\varepsilon/\varepsilon_{th}$ rather than g, γ or ε independently. We plot the minimum variance throughout the noise power spectrum as a function of the pump power which has been normalized by ε_{th} in Fig. 3. We plot variance versus frequency under different pumping power in Fig. 4.

It can be inferred from the Fig. 3 that the variance of $S_{(2)}$ would first decrease as the pump power increasing and then ascend with the pump power while $S_{(1)}$ increase as the pump power since the beginning. $S_{(2)}$ reaches its minimum value when $\varepsilon = 1.2\varepsilon_{th}$ around. Considering that $S_{(2)}$ are the short slabs of the whole entanglement model, we conclude that the $1.2\varepsilon_{th}$ is the best pump power in our case.

In Fig. 4 we investigate the relationship between entanglement intensity with pump power. As we can see from the figure, there exists a threshold and optimum value for the pump laser: if power is above the threshold, the tripartite entanglement would increase as the pump power increases at first. However, if the power continually increases over the optimal value, the entanglement intensity would decreases. Thus, these eight figures provide the insight for how to manipulate the pump power in order to obtain the maximum entanglement intensity.

6 Conclusions

In conclusion, we propose the theoretical model for the pump-signal-idler entanglement based on the high Q microresonator filled with $\chi^{(2)}$ medium. By solving Fokker-Planck equation in P representation, we analyse the entanglement case where van Loock and Furusawa criteria are violated at same time. We analytically relate the threshold of pump power with cavity parameters and find that the intensity of entanglement is completed influenced by the

$\frac{\varepsilon}{\varepsilon_{th}}$, ω/γ, and γ_c/γ. The results would offer a new path for the future study for entanglement over integrated microrresonator filled with $\chi^{(2)}$ nonlinear medium.

Acknowledgements This work is supported by the National Natural Science Foundation of China (Grant Nos. 61475099, 61102053), Program of State Key Laboratory of Quantum Optics and Quantum Optics Devices (No: KF201405), Open Fund of IPOC (BUPT) (No: IPOC2015B004), Program of State Key Information Security (No. 2016-MS-05).

References

1. Nielsen, M.A., Chuang, I.L.: Cambridge University Press (2010)
2. Lo, H.-K., Curty, M., Tamaki, K.: Nat. Photonics **8**, 595–604 (2014)
3. Jing, J., Zhang, J., Yan, Y., Zhao, F., Xie, C., Peng, K.: Phys. Rev. Lett. **90**, 167903 (2003)
4. Qin, Z., Cao, L., Wang, H., Marino, A.M., Zhang, W., Jing, J.: Phys. Rev. Lett. **113**, 023602 (2014)
5. Wang, H., Zheng, Z., Wang, Y., Jing, J.: Opt. Express **24**(20), 23459 (2016)
6. Haye, P.D., Schliesser, A., Arcizet, O., Wilken, T., Holzwarth, R., Kippenberg, T.: Nature **450**, 1214–1217 (2007)
7. Wen, Y., Wu, X., Li, R., Lin, Q., He, G.: Phys. Rev. A **91**, 042311 (2015)
8. Dutt, A., Luke, K., Manipatruni, S., Gaeta, A.L., Nussenzveig, P., Lipson, M.: Phys. Rev. Appl. **3**, 044005 (2015)
9. Chembo, Y.K., Yu, N.: Phys. Rev. A **82**, 033801 (2010)
10. Beckmann, T., Linnenbank, H., Steigerwald, H., Sturman, B., Haertle, D., Buse, K., Breunig, I.: Phys. Rev. Lett. **106**, 143903 (2011)
11. Furst, J.U., Strekalov, D.V., Elser, D., Aiello, A., Andersen, U.L., Marquardt, C., Leuchs, G.: Phys. Rev. Lett. **106**, 113901 (2011)
12. Fortsch, M., Schunk, G., Furst, J.U., Strekalov, D., Gerrits, T., Stevens, M.J., Sedlmeir, F., Schwefel, H.G., Nam, S.W., Leuchs, G., et al: Phys. Rev. A **91**, 023812 (2015)
13. Coelho, A., Barbosa, F., Cassemiro, K., Villar, A., Martinelli, M., Nussenzveig, P.: Science **326**, 823–826 (2009)
14. Ilchenko, V.S., Savchenkov, A.A., Matsko, A.B., Maleki, L.: Phys. Rev. Lett. **92**, 043903 (2004)
15. Gardiner, C.W., Collett, M.J.: Phys. Rev. A **31**, 3761 (1985)
16. Walls, D.F., Milburn, G.J.: Quantum optics. Springer Science Business Media (2007)
17. Gardiner, C.: Stochastic methods. Springer-Verlag, Berlin, Heidelberg, New York, Tokyo (1985)
18. van Loock, P., Furusawa, A.: Phys. Rev. A **67**, 052315 (2003)